

Magnetoresistances observed by decomposition of the magnetic moment in $\text{La}_{1-x}\text{Ca}_x\text{MnO}_3$ films*

Hyun-Tak Kim** and Kwang-Yong Kang

Telecom. Basic Research Lab., ETRI, Taejon 305-350, Korea

Eun-Hee Lee

Nuclear Material Technology Developments, KAERI, Taejon 305-600, Korea

A ferromagnetic phase, characterized by electron carriers and a high temperature colossal magnetoresistance (HTCMR) dependent on the magnetic moment, and a semiconducting phase, characterized by hole carriers and a low temperature CMR (LTCMR), are observed in $\text{La}_{1-x}\text{Ca}_x\text{MnO}_3$ thin films by the van der Pauw method. The LTCMR is much more sensitive to the magnetic field than the HTCMR. In the ferromagnetic phase for films with anisotropic moments in two dimensions, a remnant resistivity of the order of $10^{-8} \Omega m$ is observed up to 100 K and increases exponentially with both a temperature up to T_c and a magnetic field above one Tesla (a positive magnetoresistivity). We found that the ferromagnetic phase below T_c is in a polaronic state with a polaronic mobile conduction, and the carrier density dips near T_c . For resistances measured by the four-probe method with line electrodes, low temperature information of the HTCMR is not revealed. The van der Pauw method is more effective for the resistance measurement of a magnetic material than the four-probe method.

I. INTRODUCTION

Since the discovery of colossal (or giant) magnetoresistances (C (or G) MR)¹⁻³ for hole-doped manganese oxides $\text{La}_{1-x}(\text{Ca or Sr})_x\text{MnO}_3$, (LCMO or LSMO), the correlation between conductivity and ferromagnetism and the conduction mechanism in the ferromagnetic state have been intensively studied. The correlation is related to the strong Hund coupling between t_{2g} spins and ϵ_g electrons. For over 40 years, the coupling between the charge and the spin has been considered very important.^{4,5,6} However, some researchers have indicated that the coupling between the charge and the spin is not strong enough to describe the CMR correctly.^{7,8} They proposed local lattice distortions near T_c ^{7,8} and large oxygen isotope effects on T_c .⁹ Furthermore, the CMR mechanism is not yet fully understood.¹⁰

With regard to the conduction mechanism below T_c for LCMO or LSMO, de Gennes proposed a second double-exchange model which assumes that the charge carriers are itinerant.⁶ However, a polaronic state was suggested from observations of the resistivity and the thermoelectric power for LCMO at $x=0.12$ and 0.15, showing semiconducting behavior below T_c .¹¹ Two phases, one metallic and the other semiconducting, were separated by observing magnetoresistances for LCMO thin films.¹² A detailed review on phase separation in CMR materials was given.¹³ However, it was also suggested that the LSMO is a half metal with both metallic and semiconducting electronic structures below T_c .¹⁴ Thus, the conduction mechanism and the electronic structure for LCMO and LSMO remain unclear.

In this paper, we observe two distinct phases in LCMO films by the van der Pauw method and measure the remnant resistivity, its magnetic field dependence (a positive

MR), and the Hall coefficient in the ferromagnetic phase. The temperature dependence of Hall coefficients is presented and the results are discussed on the basis of other published results. Furthermore, for the resistance measurement of magnetic materials, the four-probe method with line electrodes is compared with the van der Pauw method with point electrodes.

II. EXPERIMENT

Thin films were deposited with a $\text{La}_{0.67}\text{Ca}_{0.33}\text{MnO}_3$ ceramic target on (100)MgO substrates at a substrate temperature of 700°C in oxygen by laser ablation. The deposited LCMO films showed semiconducting behavior for resistance before annealing. This may be attributed to the lattice mismatch between the film and the MgO substrate. The deposited LCMO films were annealed at 900°C in oxygen in a furnace and showed ferromagnetic behavior. The $\text{La}_{0.70}\text{Ca}_{0.30}\text{Mn}_{0.97}\text{O}_3$ (LCMO2/12H), $\text{La}_{0.63}\text{Ca}_{0.36}\text{Mn}_{1.17}\text{O}_3$ (LCMO3/1H), and $\text{La}_{0.67}\text{Ca}_{0.33}\text{Mn}_{1.07}\text{O}_3$ (LCMO8/10H) films were annealed for twelve, one, and ten hours, respectively. Their dimensions were $3 \times 4 \text{ mm}^2$, $3.3 \times 3.7 \text{ mm}^2$, and $3 \times 3 \text{ mm}^2$, respectively, and the thicknesses were 3800 Å, 2500 Å, and 4080 Å, respectively. In our notation LCMOn/mH, n and m denote the number of the samples and annealing time, respectively. Chemical contents of the films were revealed by electron probe microanalysis. Ca was distributed homogeneously in the films. The films were oriented along the c-axis by an X-ray diffractometer. After annealing films for more than 4 hours, the full width at half-maximum of the X-ray diffraction peaks was less than that before annealing. The oxygen content and crystalline order might be optimized by gradually varying the

annealing time. For measuring magnetoresistances, electrodes were attached to four edges of the film with a square structure and denoted by marks A, B, C and D in a clockwise manner. When the current flows from A to B (x-axis), the voltage is measured at D and C (ρ_{xx}); when the current flows from B to C (y-axis), the voltage is measured at A and D (ρ_{yy}). The axis direction is arbitrary for any film. The above procedure is known as the van der Pauw method. Hall coefficients were measured along the diagonal direction orthogonal to the current flow.¹⁵ The magnetic field was applied along the c-axis of the films in a SQUID of Quantum Design Co.. We used a Hewlett Packard nanovoltmeter in this study.

III. RESULTS AND DISCUSSION

In a previous paper,¹² we found a low-temperature colossal magnetoresistance (or resistivity) (LTCMR) with peaks at 90 K and a high-temperature colossal magnetoresistance (or resistivity) (HTCMR) with peaks at $T_c=210$ K in the LCMO3/1H film, as shown in Fig. 3 (a) and (b). Here, the HCTMR depends on the ferromagnetic moment. We found that with an increasing annealing time the LTCMR decreases and the HCTMR develops; this is due to the canting behavior of the moment.¹² The two CMR's are characteristic of the respective phases in assuming two phases. The two phases were not distinguishable by X-ray diffraction because of the high crystallinity of the thin films.

Figure 1 shows resistivities measured by the van der Pauw method with 50 μ A at 0 and 5 Tesla for the LCMO8/10H film. The resistivities with peaks at $T_c=170$ K and 200 K correspond to the x-HCTMR induced by the x-component \overrightarrow{M}_x of the projection \overrightarrow{M}_{xy} on to the $x - y$ plane of a magnetic moment \overrightarrow{M} . This is because the peak temperatures agree closely with the temperature where \overrightarrow{M}_z goes to zero, as shown in the inset of Fig. 1. Below 100 K, remnant resistance voltage and resistivity were measured at 0 Tesla and were found to be, on average, 3 μ V and 10^{-3} $m\Omega cm$ (or 10^{-8} Ωm), respectively. These values are regarded as constant with temperature, although there is low-level noise. The resistivity is of the same order as that for a $Y_{0.7}Sr_{0.3}MnO_3$ thin film.¹⁶ The resistivity below 100 K increases slightly at 5 Tesla, as indicated by A in the figure. The logarithmic resistivities are linear from 100 K to T_c , which indicates nearest-neighbour hopping of polarons, as suggested by Hundley et al.¹⁷ For the resistivity measured at 0 Tesla, in assuming $\rho \propto \exp(-E/k_B T)$ which is different from the hopping term for semiconductors, E is estimated at 157 meV below T_c . This indicates that charges below the Fermi energy contribute to conduction. The mechanism of the conduction is still unclear below 100 K. The y-HCTMR peaks D and E in Fig. 1 are overlapped by the negative LTCMR values on the order of $10^1 - 10^0$ $m\Omega cm$ of peaks B and C below 150

K. Therefore, the y-HCTMR cannot be determined exactly and might not be equal to the x-HCTMR. Peaks at B and D are indistinguishable due to overlapping H and LTCMR. Generally, the HCTMR decreases as the magnetic moment increases.^{17,18} Here, the y-HCTMR is measured along the y-axis and induced by \overrightarrow{M}_y .

In order to obtain the Hall voltage of the HCTMR, we made a LCMO2/12H film. Magnetoresistance voltages (V_{xx} and V_{yy}) and the Hall voltage V_{xy} were measured at 5 Tesla from 5 to 400 K by the van der Pauw method, as shown in Fig. 2(a). The resistivities with a peak at 160 K correspond to the HCTMR revealed by the magnetic moment, as shown elsewhere¹². The LTCMR was undetectably low. Two HCTMRs nearly agree, which indicates that the magnetic moment is nearly isotropic ($\overrightarrow{M}_x \approx \overrightarrow{M}_y$). Below 50 K, resistivities are of the order of $10^{-1} - 10^{-2}$ $m\Omega cm$, which are much larger than the order of 10^{-8} $m\Omega cm$ for LCMO8/10H in Fig. 1. These larger resistivities occur because (1) the x-HCTMR when $\overrightarrow{M}_x = \overrightarrow{M}_y$ is larger than the x-HCTMR when $\overrightarrow{M}_x > \overrightarrow{M}_y$, and (2) the positive MR competes with the negative LTCMR depressed undetectably at low temperatures.

The Hall coefficient, R_H , and the carrier density measured at 5 Tesla for the LCMO2/12H film are shown in the inset of Fig. 2 (b). The negative value of the R_H indicates that carriers are electrons which are regarded as d -electrons. The R_H shows two peaks, and the peak at 140 K corresponds to T_c in the resistivity in Fig. 2. The transition range from 140 to 230 K is due to the Hall voltage variation near T_c , as shown in Fig. 2 (a). Above 230 K in the paramagnetic region, the R_H decreases with an increasing temperature. This is the same result obtained by Jaime et al.¹⁹, suggesting small polaron conduction. Below $T_c=140$ K in the ferromagnetic region with a decreasing temperature, the R_H decreases, which indicates that the carrier density increases as shown in Fig. 2 (b). The increase of the carrier density results in a decrease of resistivity with a decreasing temperature, which is not characteristic of the metallic state but instead is suggestive of a condensed state with a polaronic conduction. This suggestion is consistent with the results obtained by optical methods^{20,21} and a photoemission experiment²⁰. At T_c , the R_H has a peak, indicating a carrier density collapse which is the cause of the HCTMR, as suggested by Alexandrov and Bratkovsky²³. The carrier density of 1.3×10^{18} cm^{-3} at 5 K was calculated by assuming that the effective mass is equal to the bare electron mass. The absolute value of the carrier density is uncertain because the effective mass of the carrier could not be evaluated accurately. In the polaron case the effective mass is larger than the bare mass; moreover, for the LCMO9/15H a negative R_H was also observed. The negative R_H is consistent with negative thermopower as measured in a thin film of $La_{0.67}Ca_{0.33}MnO_3$ fabricated by a simple metalorganic decomposition technique²⁴, but it contrasts with Asamitsu and Tokura's result²⁵ and that of Cao *et al.*²⁶ in which the carriers are holes at very low temperatures

below T_c . Furthermore, it was reported that the Mn_{3d} band with electrons increases near the Fermi energy and that the O_{2p} peak with holes decreases as the photon energy increases in the photoemission experiment; this supports the negative R_H .²⁷ Therefore, for LCMO2/12H and LCMO9/15H films the measurement of the negative R_H indicates that the value of the LTCMR rather than the HTCMR is considerably lower. Here, in measuring the R_H , the resistance measured along the applied current direction was negative, which indicates that the R_H is caused by the anomalous Hall coefficient which is generally larger than the ordinary Hall coefficient for ferromagnetic materials.

We now discuss comments on Cao *et al.*'s Hall-measurement data²⁶ on which Ziese²⁸ commented. Cao *et al.*²⁹ responded to Ziese's comment. Effects of two phases in Cao's R_H data were not separated completely because the R_H was determined by Hall resistance in a ρ_{xy} (or diagonal) direction. In this case, when the sample is annealed at 900°C for at least 10 hours, the R_H can become negative at low temperatures far below T_c . Cao's suggestion, which includes two types of conduction mechanisms in LCMO , can be explained by introducing a two-phase concept, as suggested in this paper. However, Ziese did not mention a two-phase concept in his comment. The analysis of data in which effects of two phases are merged is very complicated as Ziese mentioned. For our analysis, we selected data obtained from 30 samples.

For the LCMO3/1H film, the LTCMR, x -HTCMR, positive MR, and R_H are shown in Fig. 3. Magnetoresistances, ρ_{xx} and ρ_{yy} , were measured with 50 μA from 5 to 400 K by the van der Pauw method. The LTCMR in ρ_{yy} measured along the y -axis with a peak at 90 K and the x -HTCMR with a peak at 210 K are well separated, as shown in Figs. 3 (a) and (b). The LTCMR in ρ_{yy} is much more sensitive to the magnetic field than the HTCMR. Evidently the y -HTCMR was overshadowed by the LTCMR in Fig. 3 (b). With a 500 μA current flow through the film, a screened y -HTCMR approximately three times the size of the x -HTCMR was observed near 250 K in Fig. 4 (b). This indicates that the film has two phases and that the magnetic moment is anisotropic. Peak positions of the HTCMR in Fig. 4 shifted from 210 K to 250 K, though the positions did not shift. Identifying the cause of the shift remains an open problem in this paper. The LTCMR is reduced with an increasing annealing time but does not disappear because it might have arisen from a non-perfect crystalline order due to a dislocation, a defect, an oxygen deficiency or compositional inhomogeneity.¹² For example, Jaime *et al.*³⁰ measured the HTCMR without the LTCMR but also observed a thermopower peak near 150 K corresponding to an LTCMR for a MN6/48H film deposited with a $\text{La}_{0.67}\text{Ca}_{0.33}\text{MnO}_3$ target by laser ablation on MgO and annealed in oxygen for 48 hours, as shown in Fig. 3 in their paper³⁰. Moreover, by the four-probe method with line electrodes for LCMO3/1H , the HTCMR, which depends on the ferromagnetic moment, was not found but

instead the LTCMR was observed. This indicates that the HTCMR was screened by the LTCMR because the HTCMR is much smaller than the LTCMR as shown in Figs. 3 (a) and (b).

Figure 3 (c) shows the R_H obtained by the van der Pauw method in the diagonal direction of the film. The shape of the R_H is similar to that of the LTCMR in Fig. 3 (b). No effect of the HTCMR is seen because the small Hall voltage is screened by the large Hall voltage induced by the LTCMR. The positive value of the R_H indicates that carriers are holes and corresponds to the ordinary Hall coefficient because the semiconducting phase is not ferromagnetic. The carrier density of approximately $1.2 \times 10^{15} \text{ cm}^{-3}$ at 90 K increased exponentially up to $2.2 \times 10^{17} \text{ cm}^{-3}$ at 400 K. These densities were calculated by assuming that the effective mass is equal to the bare electron mass. The activation energy of the resistivity is 61 meV which is calculated from the R_H data from 90 K to 400 K in Fig. 3 (c). This energy, due to excitation by thermal phonons, can not be observed by optical methods. Thus, the activation energy is not a broad mid-infrared peak observed by optical methods^{20,21} and a minority spin gap ($\approx 0.6 \text{ eV}$) observed by spin-resolved photoemission¹⁴, but instead corresponds to a pseudogap. Calculated from the resistivity and the R_H measured at 5 Tesla, the mobility is below $4 \text{ cm}^2/\text{Vs}$ and decreases overall with an increasing temperature except for a broad convex curvature near 160 K, as shown in the inset of Fig. 3 (c). This indicates that the conduction is polaronic below and above 90 K. The polaronic state observed by Zhou *et al.*¹¹ corresponds to this LTCMR with hole carriers.

Figure 3 (d) shows remnant resistivities measured along the x -axis as a function of field at \pm field at 5 K and 90 K. The resistivities are of the order of $10^{-3} \text{ m}\Omega\text{cm}$ (or $10^{-8} \Omega\text{m}$) below 100 K, as indicated by A in Fig. 3 (a). They are nearly constant below 1 Tesla and increase with an increasing field above 1 Tesla (positive MR), except for peaks near 400 Oe for resistivities at 90 K. This positive MR is the same as that observed for the LCMO8/10H as shown at A in Fig. 1.

Figure 5 shows temperature dependences of resistances measured along the x -axis and y -axis by the four-probe method with line electrodes without magnetic field for an LSMO/MgO film deposited with a $\text{La}_{0.67}\text{Sr}_{0.33}\text{MnO}_3$ target by laser ablation. The current between electrodes was 50 μA . The film was not annealed at a high temperature. The dimension of the film was $5 \times 5 \text{ mm}^2$. The resistance ρ_{xx} was measured along the x -axis by the four-probe method with the y -axis-line electrodes deposited with gold, as shown in the inset of Fig. 5. After measuring ρ_{xx} , the gold electrodes on the film were removed with an etchant KI (Potassium Iodine) solution. The surface of the film might have been slightly damaged, but the damage was not obvious. After removing the y -axis-line electrodes completely, the x -axis-line electrodes were deposited to measure ρ_{yy} . The resistance ρ_{yy} was measured along the y -axis by the same method as ρ_{xx} .

The resistances have peaks A and C near 70 K corresponding to the LTCMR and peaks B and D near 150 K corresponding to the HTCMR. The peaks of the HTCMR were screened below 100 K by the peaks of the LTCMR. Thus, low temperature information of the HTCMR is not revealed here. This is different from the resistances shown in Fig. 1, Figs. 3 (a) and (b), and Fig. 4.

The two-phase concept was introduced to justify the van der Pauw method. This concept has generally been accepted for oxide materials. Some examples have been suggested as follows. Scanning tunneling microscopy observed microscopic electronic inhomogeneity on the surprisingly short scale of approximately 30\AA for high- T_c superconductors.³¹⁻³³ Metal-insulator instability³⁴ near an optimal doping was theoretically found. Heat capacity anomalies for strongly correlated metals were explained by means of measurement.³⁵ Many papers reported the phase separation in CMR materials,¹³ which indicate that the existence of two phases is intrinsic. Therefore, the four-probe method with line electrodes, measuring the resistance where the two-phase effects of metallic and semiconducting properties are merged, is less effective for magnetic materials than the van der Pauw method which is known to be applicable to homogeneous materials.

IV. CONCLUSION

When magnetic moments are anisotropic and current flows along a direction with a large spin polarization, the resistivity of the ferromagnetic phase reaches a minimum. However, the minimum resistivity is screened by the LTCMR when the LTCMR and the HTCMR are not separated.

The semiconducting phase of the LTCMR is regarded as an impurity phase imbedded in the ferromagnetic phase with the HTCMR. Thus, this LTCMR phase is attributed not to the semiconducting electronic structure predicted in a half-metallic electronic structure¹⁴ but to the remnant phase due to the metal-insulator instability near an optimal doping³³.

The low resistivity, the positive CMR, and the non-metallic temperature dependence of both the resistivity and the Hall coefficient below T_c indicate that ferromagnetic conduction is not governed by free carriers, but instead by mobile polarons condensed by an attractive potential energy due to a strong electron-phonon interaction known as the Jahn-Teller effect⁷.

Other possibilities for condensation of the ferromagnetic phase have been presented as follows. A structure-phase transition with a magnetic transition, caused by a large breathing-mode distortion, was observed.⁸ Electronic specific heat anomalies were observed for a ceramic $\text{La}_{0.67}\text{Ca}_{0.33}\text{MnO}_3$ by Ramirez et al al.³⁶ and $\text{La}_{0.8}\text{Ca}_{0.2}\text{MnO}_3$ by Tanaka and Mitsuhashi³⁷, who suggested the anomaly was evidence of a second-order transition. The density of states (DOS) of the ferromagnetic

phase, as the conductance of a tunnel junction, was measured for $\text{La}_{0.67}\text{Sr}_{0.33}\text{MnO}_3$ at 4.2 K by Yu Lu et al.³⁸ (see FIG. 3 in Yu Lu's paper). The DOS has a parabolic shape within $\pm 0.2\text{V}$ and V shape within $\pm 0.05\text{V}$ regarded as the effect of LTCMR, indicating that when the effect of LTCMR is removed, quasiparticles (or carriers) exist not near the Fermi surface but below it. The same experimental result was also observed by high resolution photoemission spectroscopy by Park et al.³⁹ (see FIG. 3(c) in Park's paper). The parabolic DOS is similar to the DOS of a ferromagnet^{40,41}, a half metal^{40,41}, and a p-wave superconductor as the ABM state⁴².

Furthermore, we suggest that both the LTCMR and the van der Pauw method can be applied to a magnetoresistance sensor.

ACKNOWLEDGEMENTS

We acknowledge Ms. Juli Scherer as an editorial supervision of the ETRI journal for proofreading.

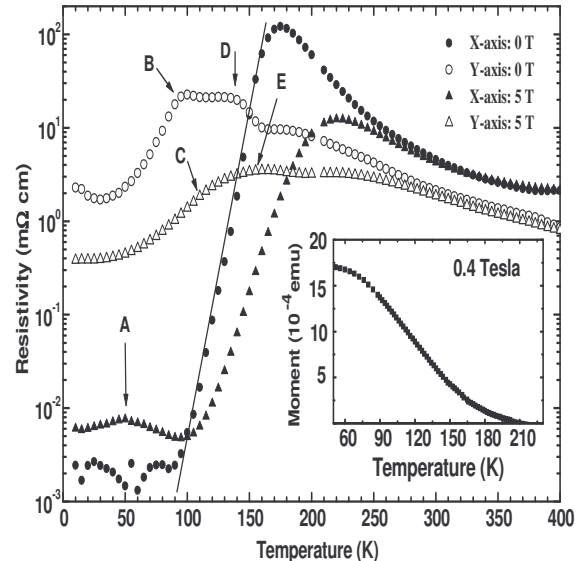


FIG. 1. Temperature and magnetic field dependencies of magnetoresistivities for the LCMO8/10H film. The inset shows the temperature dependence of the z-axis magnetic moment.

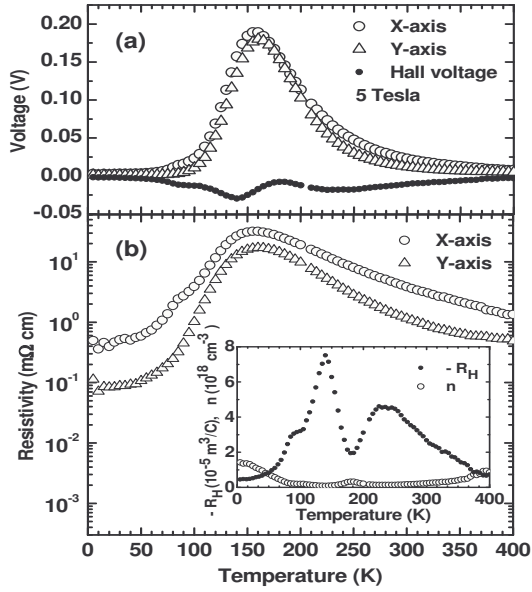


FIG. 2. (a) Temperature dependencies of resistance and Hall voltages for the LCMO2/4H film. (b) Temperature and magnetic field dependencies of magnetoresistivities. The inset in Fig. (b) shows the Hall coefficient and the carrier density.

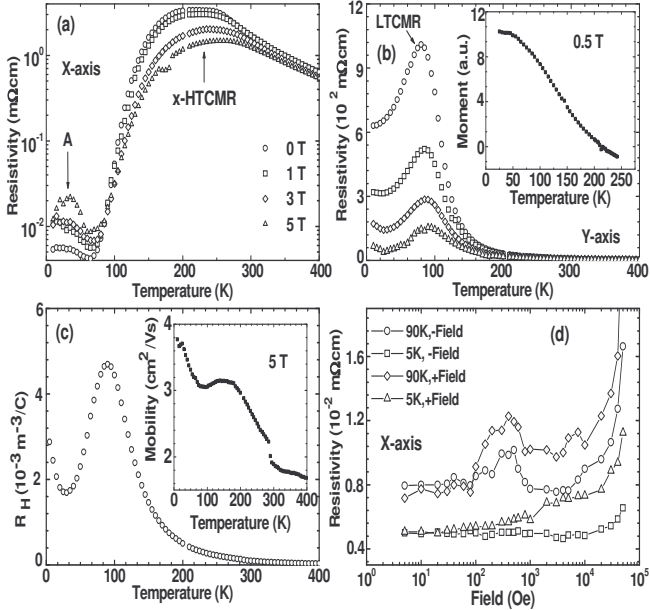


FIG. 3. (a) and (b) Temperature and magnetic field dependencies of magnetoresistivities for the LCMO3/1H film. The inset in Fig. (b) shows the temperature dependence of the magnetic moment. (c) Temperature dependencies of the Hall coefficient. The inset in Fig. (c) shows the mobility. (d) Magnetic field dependencies of magnetoresistivities measured at \pm fields at 5 K and 90 K for the LCMO3/1H film.

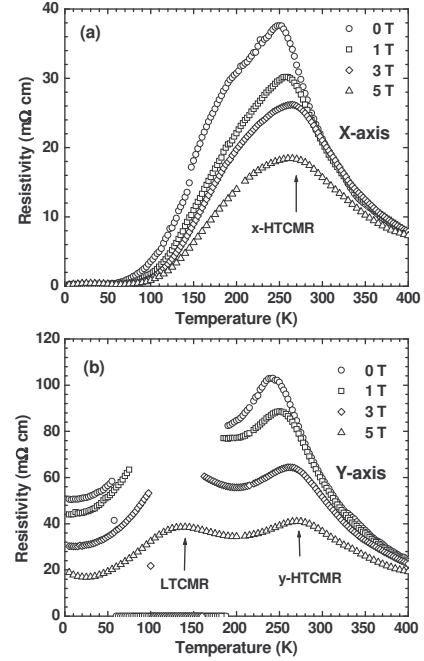


FIG. 4. Temperature and magnetic field dependencies of magnetoresistivities measured with $500 \mu\text{A}$ current for the LCMO3/1H film. (a) Peaks corresponding to the x-HTCMR. (b) Peaks near 250 K and 100 K in Fig. (b). (b) correspond to the y-HTCMR and LTCMR, respectively. Some data at fields of 0, 1 and 3 Tesla near 100 K in Fig.(b) could not be measured because of a measurement limit of a voltmeter at $500 \mu\text{A}$.

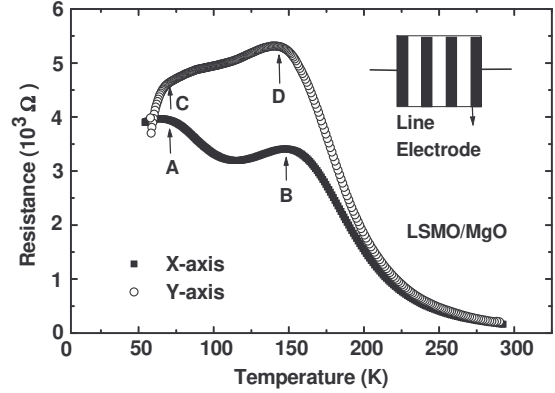


FIG. 5. Temperature dependences of resistances measured by the four-probe method with line electrodes at 0 Tesla with flowing $50 \mu\text{A}$ for the LSMO/MgO film. Peaks B and D correspond to the x-HTCMR and y-HTCMR, respectively. Peaks A and C correspond to the LTCMR.

* In printing, J. Appl. Phys., June 1, 2002.

** kimht45@hotmail.com: htkim@etri.re.kr.

¹ K. Chahara, T. Ono, M. Kasai, and Y. Kozono, Appl. Phys. Lett. **63**, 1990 (1993).

² R. von Helmolt, J. Wecker, B. Holzapfel, L. Schultz, and K. Samwer, Phys. Rev. Lett. **71**, 2331 (1993).

³ Y. Tokura, A. Urushihara, Y. Moritomo, T. Arima, A. Asamitsu, A. Kito, and H. Furukawa, J. Phys. Soc. Jpn. **63**, 3931 (1994).

⁴ C. Zener, Phys. Rev. **82**, 403 (1951).

⁵ P. W. Anderson and H. Hasegawa, Phys. Rev. **100**, 675 (1955).

⁶ P. G. de Gennes, Phys. Rev. **118**, 141 (1960).

⁷ A. J. Millis, P. B. Littlewood, and B. I. Shraiman, Phys. Rev. Lett. **74**, 5114 (1995); Phys. Rev. **77**, 175 (1996).

⁸ D. N. Argyriou, J. F. Mitchell, C. D. Potter, D. G. Hinks, J. D. Jorgensen, and S. D. Bader, Phys. Rev. Lett. **76**, 3826 (1996).

⁹ G. Zhao *et al.*, Nature (London) **381**, 676 (1996).

¹⁰ Y. Tokura, J. Magn. Magn. Mater. **200**, 1 (1999).

¹¹ J.-S. Zhou, J. B. Goodenough, A. Asamitsu, and Y. Tokura, Phys. Rev. Lett. **79**, 3234 (1997).

¹² Hyun-Tak Kim, M. Nasir Khan, and H. Uwe, J. Korean Phys. Soc. **32**, S1497 (1998).

¹³ E. Dagotto, T. Hotta, and A. Moreo, <http://xxx.lanl.gov/abs/cond-mat/0012117>.

¹⁴ J.-H. Park, E. Vescovo, H. -J. Kim, C. Kwon, R. Ramesh, and T. Venkatesan, Nature (London) **392**, 794 (1998).

¹⁵ L. J. van der Pauw, Philips Res. Rep. **13**, 1 (1958).

¹⁶ J. M. D. Coey, A. E. Berkowitz, Ll. Balcells, and F. F. Putris, Phys. Rev. Lett. **75**, 3910 (1995).

¹⁷ M. F. Hundley, M. Hawley, R. H. Heffner, Q. X. Jia, J. J. Neumeier, J. Tesmer, J. D. Thompson, and X. D. Wu, Appl. Phys. Lett. **67**, 860 (1995).

¹⁸ K. Kubo and N. Ohata, J. Phys. Soc. Jpn. **33**, 21 (1972).

¹⁹ M. Jaime, H. T. Hrdner, M. B. Salamon, M. Rubinstein, P. Dorsey, and D. Emin, Phys. Rev. Lett. **78**, 951 (1997).

²⁰ Y. Okimoto, T. Katsufuji, T. Ishikawa, T. Arima, and Y. Tokura, Phys. Rev. B **55**, 4206 (1997).

²¹ K. H. Kim, J. H. Jung, and T. W. Noh, J. Korean Phys. Soc. **32**, S1832 (1998).

²² J.-H. Park, C. T. Chen, S. W. Cheong, W. Bao, G. Meigs, V. Chakarian, and Y. U. Idzerda, Phys. Rev. Lett. **76**, 4215 (1996).

²³ A. S. Alexandrov and A. M. Bratkovsky, Phys. Rev. Lett. **82**, 141 (1999).

²⁴ Baoxing Chen, C. Uher, D. T. Morelli, J. V. Manstese, A. M. Mance, and A. L. Michel, Phys. Rev. B **53**, 5094 (1996).

²⁵ A. Asamitsu and Y. Tokura, Phys. Rev. B **58**, 47 (1998).

²⁶ X. W. Cao, J. Fang, Z. H. Wang, and K. B. Li, Appl. Phys. Lett. **75**, 3372 (1999).

²⁷ T. Takeuchi *et al.*, 1998 Autumn Meeting Abstracts of the Physical Society of Japan, Vol. **53**, Issue 2, Part 2, p 224, No. of Presentation 26a-YP-4 (Japanese).

²⁸ M. Ziese, Appl. Phys. Lett. **76**, 3653 (2000).

²⁹ X. W. Cao, J. Fang, Z. H. Wang, and K. B. Li, Appl. Phys. Lett. **76**, 3654 (2000).

³⁰ M. Jaime, M. B. Salamon, K. Pettit, M. Rubinstein, R. E. Treece, J. S. Horowitz, and D. B. Chrisey, Appl. Phys. Lett. **68**, 1576 (1996).

³¹ T. Cren, D. Roditchev, W. Sacks, J. Klein, J.-B. Moussy, C. Deville-Cavellin, and M. Lagues, Phys. Rev. Lett. **84**, 147 (2000).

³² T. Cren, D. Roditchev, W. Sacks, and J. Klein, Europhys. Lett. **54** (1), 84 (2001).

³³ S. H. Pan, J. P. O'Neal, R. L. Badzey, C. Chamon, H. Ding, J. R. Engelbrecht, Z. Wang, H. Eisaki, S. Uchida, A. K. Gupta, K.-W. Ng, E. W. Hudson, K. M. Lang, and J. C. Davis, Nature **413**, 282 (2001).

³⁴ Hyun-Tak Kim, Phys. Rev. B **54**, 90 (1996).

³⁵ Hyun-Tak <http://xxx.lanl.gov/abs/cond-mat/0110112>.

³⁶ A. P. Ramirez, P. Schiffer, S.-W. Cheong, C. H. Chen, W. Bao, T. T. M. Palstra, P. L. Gammel, D. J. Bishop, and B. Zegarski, Phys. Rev. Lett. **79**, 3188 (1996).

³⁷ J. Tanaka and T. Mitsuhashi, J. Phys. Soc. Jpn. **53**, 24 (1984).

³⁸ Yu Lu, X. W. Li, G. Q. Gong, G. Xiauo, A. Gupta, P. Lecoeur, J. Z. Sun, Y. Y. Wang, and V. P. Dravid, Phys. Rev. B **54**, R8357 (1996).

³⁹ J.-H. Park, C. T. Chen, S.-W. Cheong, W. Bao, G. Meigs, V. Chakarian, and Y. U. Idzerda, Phys. Rev. Lett. **76**, 4215 (1996).

⁴⁰ A. M. Bratkovsky, Phys. Rev. B **56**, 2344 (1997).

⁴¹ A. M. Bratkovsky, Appl. Phys. Lett. **72**, 2334 (1998).

⁴² M. Sigrist and K. Ueda, Rev. Mod. Phys. **63**, 239 (1991).